

Articles

Comparison of N-Terminal Modifications on Neurotensin(8–13) Analogues Correlates Peptide Stability but Not Binding Affinity with in Vivo Efficacy

Kevin S. Orwig,[†] McKensie R. Lassetter,[†] M. Kyle Hadden,[†] and Thomas A. Dix^{*,†,‡}*Department of Pharmaceutical Sciences, Medical University of South Carolina, 280 Calhoun Street, P.O. Box 250140, Charleston, South Carolina 29425, Argolyn Bioscience Inc., 530 Meridian Parkway, Suite 200, Durham, North Carolina 27713*

Received August 28, 2008

Neurotensin(8–13) and two related analogues were used as model systems to directly compare various N-terminal peptide modifications representing both commonly used and novel capping groups. Each N-terminal modification prevented aminopeptidase cleavage but surprisingly differed in its ability to inhibit cleavage at other sites, a phenomenon attributed to long-range conformational effects. None of the capping groups were inherently detrimental to human neurotensin receptor 1 (hNTR1) binding affinity or receptor agonism. Although the most stable peptides exhibited the lowest binding affinities and were the least potent receptor agonists, they produced the largest in vivo effects. Of the parameters studied only stability significantly correlated with in vivo efficacy, demonstrating that a reduction in binding affinity at NTR1 can be countered by increased in vivo stability.

Introduction

As the natural mediators and regulators of numerous physiological processes, peptides possess vast therapeutic potential. However, the pharmaceutical use of peptides is encumbered by several factors including their inability to cross biological barriers, variable selectivity, and instability in biological matrices primarily due to degradation by peptidases. A variety of strategies have been explored to address these issues including the use of targeted delivery methods,¹ conjugation,^{2,3} peptide prodrugs (e.g., cyclization),⁴ reduced peptide bonds,⁵ and numerous other backbone modification schemes.^{6–10} These approaches suffer from either a lack of generality or often lead to a reduction in affinity and/or potency via perturbation of the active peptide conformation or alteration of essential functional groups. Alternatively, chemical modifications of peptide termini are commonly employed to block exopeptidase activity. This strategy is simple, broadly applicable, and improves peptide biostability without altering the backbone and side chain functional groups necessary for full biological activity.¹¹ Aminopeptidases are the major source of proteolytic activity in most tissues, and their action represents the predominant degradation pathway for peptides containing a free N-terminal amine, even in the presence of an unprotected carboxyl terminus.^{12–15} Protection of the N-terminus is therefore essential to peptide stability in vivo, and methods such as N-terminal acetylation and methylation have found widespread use.^{14,16–19} Additionally, our laboratory has observed that N-terminal substitution with α -azido acids, methyl groups, or hydrogen atoms substantially increased peptide biostability, hydrophobicity, and activity in various peptide models without adversely affecting other pharmacokinetic properties.^{20–22} This suggests that incorpora-

tion of appropriate N-terminal modifications may have the potential to improve a greater range of peptide characteristics than currently recognized. However, direct comparisons between N-terminal modifications with respect to a variety of pharmacokinetic (PK^a) parameters have not been reported, which is the subject of this report.

To examine this issue, we selected the hexapeptide NT(8–13) (**1**), the active fragment of neurotensin (NT), as a pharmaceutically relevant model system. NT has a number of biological activities both in the central nervous system and the periphery, and NT derivatives have been studied as potential antipsychotics, analgesics, and tumor-targeting compounds.^{23–25} Thus, **1** has been extensively studied and its cleavage pattern well documented. Furthermore, N-terminally modified analogues of **1** have been developed and characterized. We studied the effect of six N-terminal capping groups (amino-, *N*^α-acetyl-, *N*^α-methyl-, *C*^α-methyl-, azido-, and hydro-) on a variety of PK parameters in **1** and two related analogues, KH28²² (**11**) and the Eisai hexapeptide²⁶ (**15**) (Table 1). Because **1**, **11**, and **15** all act at the same receptor to elicit the same biological responses, this set of peptides provides an ideal system for this study. Three series of N-terminal derivatives based on **1**, **11**, and **15** were synthesized. Peptides in each series featured each of the six capping groups at the N-terminal α -carbon in place of the α -amine (Table 1). As an initial comparison, we studied how these N-terminal groups influenced peptide stability, receptor binding affinity, Ca²⁺ mobilization, and in vivo efficacy. Our results demonstrate that relatively minor modifications at peptide N-termini can make dramatic contributions to the overall PK

* To whom correspondence should be addressed. Phone: (843) 876-5092. Fax: (843) 792-1617. E-mail: dixta@musc.edu.

[†] Department of Pharmaceutical Sciences, Medical University of South Carolina.

[‡] Argolyn Bioscience Inc.

^a Abbreviations: NT, neurotensin; hNTR1, human neurotensin receptor 1; BBB, blood–brain barrier; Hlys, homolysine; ip, intraperitoneal; MALDI-TOF, matrix-assisted laser desorption ionization time-of-flight; MTBE, methyl-*tert*-butyl ether; Mtr, 4-methoxy-2,3,6-trimethylbenzenesulfonyl; NN, neuromedin N; NT, neurotensin; NTR, neurotensin receptor; Pbf, 2,2,4,6,7-pentamethylbenzofuran-5-sulfonyl; PK, pharmacokinetic; SAR, structure–activity relationship; X_p, (S)-(–)-4-(phenylmethyl)-2-oxazolidinone.

Table 1. Designations, N-Terminal Moieties, and Primary Sequences of the Peptides Included in This Study

peptide series	compd no.	N-terminus ^a	peptide designations					
			primary sequence position ^b					
			8	9	10	11	12	13
NT(8–13)	1	amino –	Arg	Arg	Pro	Tyr	Ile	Leu
	2	acetyl–						
	3	<i>N</i> ^α -methyl–						
	4	azido–						
	5	<i>C</i> ^α -methyl–						
	6	des-amino–						
KH28	7	amino–	HLys ^c	Arg	Pro	Tyr	Tle	Leu
	8	acetyl–						
	9	<i>N</i> ^α -methyl–						
	10	azido–						
	11	<i>C</i>^α-methyl –						
	12	des-amino–						
Eisai	13	amino–	Arg	Lys	Pro	Trp	Tle	Leu
	14	acetyl–						
	15	<i>N</i> ^α - methyl –						
	16	azido–						
	17	<i>C</i> ^α -methyl–						
	18	des-amino–						

^a Boldface type indicates the native N-terminal group for the parent peptide in each series. ^b Numbering of primary sequence is relative to full-length neurotensin(1–13). ^c HLys is homolysine.

profile and implicate peptide biostability as the major parameter impacting biological response in the NT system.

Experimental Section

Peptide Synthesis. Peptides were synthesized manually using Merrifield solid-phase methodology as previously reported.^{20,27} All amino acids were the Fmoc-protected²⁸ L forms and were purchased from commercial sources unless otherwise noted. N-acetylated peptides (**2**, **8**, and **14**) were prepared by stirring Fmoc-deprotected peptidyl resin with a solution composed of 10% pyridine and 10% acetic anhydride in DMF for 20 min. Commercially available *N*^α-methylated Arg (Boc-*N*^α-Me-Arg(Mtr)-OH) was used to prepare both **3** and **15**. N-terminally modified non-natural residues for incorporation at position 8 of peptides **4–6**, **7–12**, and **16–18** (Table 1) were synthesized in-house as detailed below. Where applicable, optical purity at the α-carbon for synthesized amino acids was determined to be ≥95% by following azide or methyl addition in the presence of the chiral auxiliary.^{29,30} Crude peptides were purified by preparative HPLC using a Waters radial compression column (PrepLC 25 mm module containing a NovaPak C₁₈ 60 Å cartridge) with a gradient from 5 to 40% CH₃CN in H₂O (+0.1% TFA) over 40 min. Pure peptides were lyophilized, and structure and purity were confirmed by analytical HPLC and MALDI-TOF analysis.

Synthesis of N-Terminally Modified Residues. *N*^ω-Pbf-(2*S*)-5-Guanidino-2-azidovaleric Acid (19**).** Fmoc-Arg(Pbf)-OH (**20**) (6.5 g, 10.0 mmol) was stirred in 10% piperidine in MeOH for 20 min and then dried under reduced pressure. The resulting white powder was redissolved in pH 5.0 H₂O (50 mL) and extracted with CH₂Cl₂ (3 × 50 mL). The aqueous layer was dried in vacuo, resulting in 4.27 g of a white crystal (**21**) (99% yield) that was used without further purification. The free α-amino group of **21** was then converted to the azide by the diazo transfer method of Lundquist et al.³¹ The resulting residue was dried under reduced pressure and HPLC purified using a gradient of 15%–38% MeCN (+0.1% TFA) over 40 min with UV detection at 265 nm to give 4.28 g product (**19**) (94% yield) (Scheme 1, Supporting Information). Compound **19** was used to produce N₃-NT(8–13) (**4**) and N₃-Eisai (**16**).

The monomer used in the production of N₃-KH28 (**10**) was (2*S*)-2-azido-7-bromoheptanoic acid, which was coupled directly to the peptidyl resin and subsequently derivatized with excess NH₃ as described previously.²¹

The Arg analogue (2*S*)-5-guanidino-2-methylvaleric acid used to prepare *C*^α-methyl-NT(8–13) (**5**) and *C*^α-methyl-ES (**17**), and the homolysine analogue (2*S*)-7-amino-2-heptanoic acid, used to prepare *C*^α-methyl-KH28 (**11**), were synthesized as reported previously.³⁰

5-Guanidinovaleric Acid (22**).** 5-Aminovaleric acid (**23**) (6.0 g, 51.22 mmol) was dissolved in 2.0 N NaOH. *S*-methylthiourea (**24**) (12.29 g, 56.34 mmol, as the HI salt) was added and this solution stirred at 40 °C for 9 days. The reaction was dried under reduced pressure and the resulting yellow slurry purified over a Dowex-50 ion-exchange column, eluting with 1.5 N NH₄OH while monitoring by TLC (phenol:H₂O, 3:1) with bromocresol green staining. Pure fractions were combined to give 5.87 g of a white crystal (**22**) in 72% yield (Scheme 2, Supporting Information). Compound **22** was used to produce des-amino-NT(8–13) (**6**) and des-amino-Eisai (**18**).

Boc-7-aminoheptanoic Acid (25**).** 7-Bromoheptanoic acid (**26**) (10.56 g, 50.51 mmol) was dissolved in 50 mL conc NH₄OH and the solution stirred overnight at ambient temperature. The reaction was then dried under reduced pressure to give 7.26 g of a white crystal (**27**) in 99% yield. Compound **27** (7.26 g, 50.00 mmol) was dissolved in 100 mL of 10% Na₂CO₃ and 100 mL of dioxane with mild warming. Boc-O-Boc was added directly to this solution, which was then refluxed at 50 °C for 12 h. The solution was dried under reduced pressure and the residual material redissolved in 2.0 N NaOH (100 mL) and extracted with MTBE (3 × 75 mL). The aqueous layer was saved and dried to give 6.40 g of a white crystal (**25**) in 52% yield (Scheme 3, Supporting Information). Compound **25** was used to produce des-amino-KH28 (**12**).

***N*^ω-Fmoc-*N*^ω-Boc-2(*S*)-2,7-diaminoheptanoic Acid (**28**).** The Evans chiral auxiliary was removed from 5.27 g (11.83 mmol) of **29**²⁹ following the literature procedure³² to give *N*^ω-Boc-2(*S*)-7-amino-2-azidoheptanoic acid (3.37 g, 11.76 mmol) as a clear oil in 99% yield. The azide was reduced by dissolving 3.26 g (11.39 mmol) of this material in 15 mL of 1.0% CH₃COOH in MeOH in a hydrogenation flask. Next, 250 mg of palladium (Pd/C, 10 wt % on activated carbon) was added under N₂, the flask flushed with H₂, placed on a Parr reactor at 40 psi, and shaken for 12 h. The Pd/C was removed by filtration and the filtrate dried in vacuo to give 2.2 g of **30** as a white crystal in 74% yield. The α-amine of **30** was Fmoc protected following the method of Lee et al.³³ to give 4.98 g of a yellow oil **28** (85% yield) that was used without further purification (Scheme 4, Supporting Information). The

common intermediate **28** was used to prepare **7** and **8** by standard methods and **9** by following the procedure of Miller et al.³⁴

Serum Degradation Assay. Degradation rates were determined using a modified version of the method of Kokko et al.³⁵ Human or rat serum (270 μL) was placed in microcentrifuge tubes, and 30 μL of peptide analyte (10 mM in saline) was added for a final concentration of 1 mM. The tubes were incubated at 37.0 °C in a water bath. Aliquots (20 μL) were removed at predetermined times, added to 80 μL of 3:1 methanol:ethanol, immediately mixed by vortexing for 10 s, and precipitate pelleted by spinning the samples at 6000 rpm in a microcentrifuge for 10 min. Next, 1 μL of the supernatant was combined with 1 μL of quantification standard (QS, Kemptide, 0.75 mg/mL) and 4 μL of matrix (50 mM α -cyano-4-hydroxycinnamic acid (α -CHCA) in 70% MeCN and 0.1% TFA). Then 1 μL of this mixture was spotted onto a stainless steel MALDI target plate preheated to 31 °C on a hot plate. After allowing the samples to dry, the target plate was cooled to room temperature and the sample spots were analyzed using MALDI-TOF MS. Signal intensity ratios for the peptide analyte peak over the QS peak at each time point were plotted and normalized to a starting concentration of 1.0 mM by multiplying each value by the initial difference in the y-intercept. Ratios were then converted to concentrations using a standard curve generated for each compound as described below. $T_{50\text{s}}$ were calculated for each compound based on the equation for the linear regression line. Statistical significance between $T_{50\text{s}}$ was determined by a one-way repeated measures ANOVA followed by Tukey's post hoc test for multiple comparisons. Results were considered significant for $p < 0.05$.

Serum Degradation Standard Curves. A serial dilution series of each peptide analyte was constructed in both human and rat serum. All tubes in the series were maintained at 0 °C to inhibit peptidase activity. Final concentrations for each of the eight points in the series were: 2.00, 1.00, 0.750, 0.500, 0.375, 0.250, 0.125, and 0.063 mM. Working rapidly to minimize the length of time each peptide was exposed to serum, 20 μL of each concentration was removed and added to 80 μL of 3:1 methanol:ethanol. MALDI samples were then constructed as described for the degradation assay. Linear regression lines for each standard curve were normalized to a starting concentration of 1.0 mM by multiplying each value by the initial difference in the y-intercept. The standard curves for each peptide appear in Supporting Information.

Competition Binding Assay. Each assay was performed in a separate well of a nonbinding surface 96-well plate in a total reaction volume of 100 μL . Human neurotensin receptor type 1 (hNTR1) membrane preparations (Chemicon International) were diluted according to manufacturer instructions with 15.0 mL of binding buffer (50 mM HEPES, 5 mM MgCl_2 , 1 mM CaCl_2 , 0.2% BSA, pH 7.4) per mL membrane preparation. All wells received 80 μL of the diluted hNTR1 membrane preparation (2.5 $\mu\text{g}/\text{well}$), 10 μL of 5 nM ^{125}I -Tyr(3)NT (Perkin-Elmer, 0.05 Ci per assay), and 10 μL of the appropriate peptide at various concentrations (0.01 nM to 100 μM) in binding buffer. Each well was mixed by pipetting 3 \times and the assay incubated for 1 h at room temperature. The binding reactions were then terminated by dilution with 100 μL of binding buffer. The contents of each well were rapidly filtered through Whatman GF/C filters (25 mm diameter, presoaked in 0.33% polyethylenimine) using a Millipore 1225 sampling vacuum manifold and wells rinsed 3 \times each with washing buffer (50 mM HEPES, 500 mM NaCl, 0.1% BSA, pH 7.4). Each filter was immediately washed 6 \times with washing buffer and placed in tubes for γ counting. Nonspecific binding was determined in the presence of 1 μM NT(8–13), and total binding was determined in the absence of unlabeled ^{125}I -Tyr(3)NT. In a typical experiment, the specific binding was 90% or greater of the total binding. Each data point was determined in triplicate. Dose–response curves were plotted using GraphPad Prism to determine IC_{50} values. Assays were performed in duplicate with the arithmetic means reported relative to NT(8–13) \pm SE. K_i values were determined from mean $\text{IC}_{50\text{s}}$ using the Cheng–Prusoff conversion.³⁶

Measurement of Intracellular Ca^{2+} Mobilization. A FLIPR instrument (Molecular Devices) was used to measure peptide-

induced intracellular Ca^{2+} release in HT29 cells plated into 96-well microtiter plates. On the day prior to the assay, cells were seeded at approximately 100000 cells/well in 96-well clear bottom black wall microtiter plates (Becton Dickinson) and grown overnight in a CO_2 incubator at 37 °C. On the day of the assay, cells (at approximately 90% confluency) were loaded with 4 μM Fluo-3 a.m. (Molecular Probes) for 1 h in assay buffer (Hanks' balanced salt solution containing 25 mM HEPES and 2.5 mM probenecid at pH 7.4). After loading, cells were washed 3 \times using Hanks' balanced salt solution on an automated plate washer (Labsystems) and placed in the FLIPR. The 96 wells were simultaneously illuminated for 0.4 s by an argon laser ($\lambda = 488$ nm) set at 300 mW (Coherent Inc.). Fluorescence readings were acquired using a 540 nm band-pass filter at 5.0 s intervals for 12 readings to obtain a baseline measurement. Then cells were simultaneously treated with 2 μM NT(8–13) (positive control), assay buffer (negative control), or various concentrations ranging from 1.0 μM to 1.0 pM of peptide. Fluorescence readings were then acquired from each well every second for 2 min and then every 10 s for 4 min. Background fluorescence from buffer treated cells (negative controls) was removed from all tracings. Triplicate readings were averaged and normalized to the positive control. Tracings were acquired, averaged, and normalized using the FLIPR Control software (Molecular Devices). Results are reported as the means \pm SEM from triplicate determinations from at least two independent experiments. Maximal signal from the 1–3 min interval was used to generate a dose–response curve and determine an IC_{50} for each peptide using GraphPad Prism.

Hypothermia Assay. Male Sprague–Dawley Rats (250–350 g) were obtained from Harlan (Indianapolis, IN) and housed in an AAALAC-approved colony room maintained at a constant temperature and humidity. Lighting was controlled on a 12 h light:dark cycle with lights on at 0700 h. Animals were housed two per cage with ad libitum access to food and water. All experiments were performed during the light cycle. Unanaesthetized rats were restrained in Plas-Laboratories plastic cages fitted with wooden dowels to restrict movement. Rectal temperature probes (Physitemp, RET-2, Clifton, NJ), lubricated with light mineral oil, were inserted 5 cm into the rectum of each animal and connected to a microprobe thermometer (Physitemp, BAT-12) in conjunction with a thermocouple selector (Physitemp, SWT-5). Rats were allowed to acclimate to the cages for 1 h prior to ip injection. Peptides were dissolved in saline and haloperidol (4-[4-(4-chlorophenyl)-4-hydroxy-1-piperidyl]-1-(4-fluorophenyl)-butan-1-one) was dissolved in DMSO. Following the equilibration period, rats were given an ip injection of peptide (5 mg/kg), haloperidol (5 mg/kg), or saline (1 mL/kg). Initial temperature values were the average temperatures of the rats immediately before and after the injection. Subsequent measurements were taken every 30 min for 5 h. One-way repeated measures ANOVAs followed by Tukey's post hoc test for multiple comparisons were performed for each peptide using GraphPad Prism to measure statistical significance. Results were considered significant for $p < 0.05$.

Biological Results and Discussion

Prior studies established that the metabolic degradation of **1** occurs in both rats and humans at three sites resulting from the action of a suite of metalloproteases including nonspecific aminopeptidase(s) as well as endopeptidases EP 24.11 and EP 24.16 that are responsible for the primary cleavages (Figure 1).^{37–42} Cleavage at the Arg⁸–Arg⁹ and Tyr¹¹–Ile¹² sites dominates in the periphery, while cleavages between Arg⁸–Arg⁹ and Pro¹⁰–Tyr¹¹ are the major pathways in the central nervous system. The three parent peptides utilized in this study, **1**, **11**, and **15**, exhibit distinct levels of peptidase resistance and thus represent a continuum of inherent stabilities. To define the role of various N-terminal modifications in the metabolism of **1** and its derivatives, the serum stability for each N-terminally capped version of the parent scaffolds (Table 1) was measured according

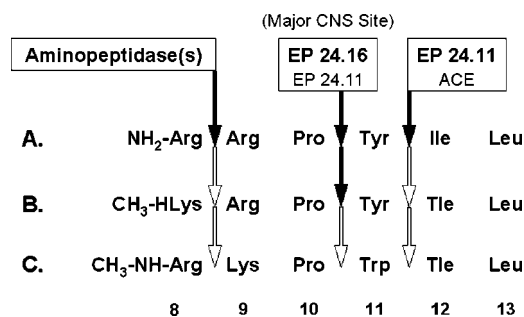


Figure 1. Primary cleavage sites as determined for the parent compound in each peptide series. (A) Cleavage pattern of NT(8–13) (**1**). (B) Cleavage pattern of KH28 (**11**) HLys represents homolysine. (C) Cleavage pattern of the Eisai hexapeptide (**15**). Enzymes (boxed) that mediate primary cleavages are in larger boldface type, those that take part in secondary cleavages are in normal type. Solid arrows depict sites of enzymatic cleavage, open arrows represent blocked cleavage sites. Sequence numbering is as denoted in Table 1.

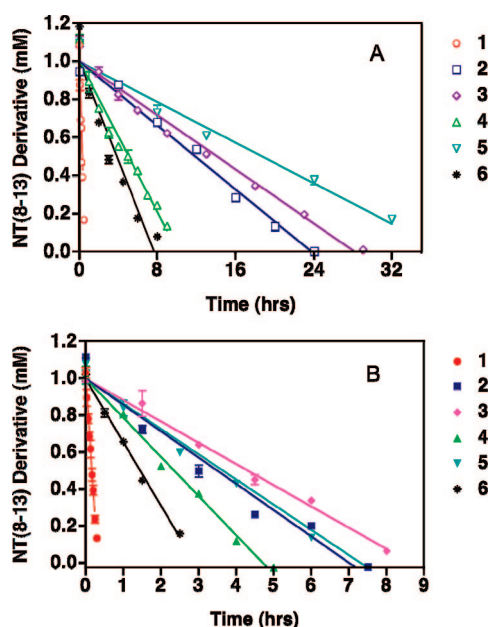


Figure 2. Comparison of degradation rates for NT(8–13) derivatives in human serum (A) and rat serum (B). Structures of compounds are as defined in Table 1. Vertical bars represent the standard error for each time point ($n = 3$).

to a quantitative MALDI-TOF MS assay, which allows simultaneous identification of degradation products by molecular mass. The serum degradation assay is conducted at relatively high concentrations (1.0 mM) of the analyte peptide in order to saturate the enzymes responsible for peptide degradation. Under these conditions, plasma peptidases do not compete for substrate utilization and the degradation rate is linear,^{15,43,44} allowing reproducible and accurate comparison between *in vitro* degradation rates. To illustrate, the degradation curves for the NT(8–13) derivatives in human and rat serum are presented in Figure 2 while the degradation rates for the three peptide series in human and rat serum are compiled in Table 2. The results demonstrate drastic differences in the degradation rates for the various N-terminally capped derivatives.

The most drastic series differences are evident in the NT(8–13) series. The half-time of disappearance, T_{50} (the time to reach 50% of the initial concentration), for this series ranges from 16.9 to 1130 min in human serum (Table 2). A similar T_{50} trend was observed in rat serum, however, the T_{50} range

was much narrower (10.0–260 min), reflecting higher rates of degradation typical of rat serum.^{15,35} Unmodified **1** degrades most rapidly in both human and rat serum with T_{50} s of 16.9 and 10.0 min, respectively. These values compare well to previous T_{50} measurements for **1** of 10–24.1 min^{35,44} in human and 5.9 min in rat serum.³⁵ The major degradation product observed (by molecular mass) for this compound was NT(9–13), corresponding to cleavage at the Arg⁸–Arg⁹ bond (Table 2). This result is consistent with other studies indicating that aminopeptidase degradation predominates for peptides lacking an N-terminal capping group.^{12–15} Degradation of all other N-terminally modified derivatives of **1** resulted in the formation of NT(8–11), corresponding to cleavage at the Tyr¹¹–Ile¹² bond, in both human and rat serum (Table 2). NT(9–13) was not detected for **2–6**, indicating that each of the N-terminal modifications was able to fully block cleavage at the Arg⁸–Arg⁹ site.

Replacement of Ile¹² with a *tert*-leucine (Tle) residue in **11** abolishes the proteolytic susceptibility of the 11–12 peptide bond (Table 2). Thus, with the exception of the N-terminally unmodified **7**, which degrades at approximately the same rate as **1**, the rates for the KH28 series are much slower and exhibit a tighter profile than those for the NT(8–13) series (Table 2). Elimination of the enzymatically preferred cleavage site at the Tyr¹¹–Ile¹² bond in **8–12** leads to slow hydrolysis at the unmodified Pro¹⁰–Tyr¹¹ bond to produce low amounts of the 8–10 fragment of **11** (Table 2).

In rat serum, the KH28 series featured a similarly narrow degradation profile. In contrast to human serum, where **10** was the most stable compound ($T_{50} = 3760$ min), its relative stability in rat serum was markedly lower ($T_{50} = 3120$ min). On the other hand, the stability of **12**, the lowest of any N-terminally modified derivative of **11** in human serum ($T_{50} = 2460$ min), increased to 4490 min, making it the most stable derivative in rat serum. Such serum-specific differences likely reflect variation between the structures of the rat and human enzymes responsible for metabolism.

The scaffold of **15** includes the Tle¹² substitution as in the KH28 series and is further substituted with a Trp residue in place of Tyr¹¹, effectively blocking all of the enzymatically labile peptide bonds (Figure 1C). The degradation profile for the Eisai peptide series (Table 2) shows both similarities and differences to the previous two series. For instance, in both human and rat serum, the N-terminally unmodified **13** degraded quickly with T_{50} s of 15.8 and 13.5 min, respectively. These values are very similar to those for **1** and **7**. Conversely, the N-terminally capped derivatives of **15** were the most stable of the three peptide series examined, with degradation rates even lower than the derivatives of **11** (Table 2). Human serum degradation curves for **14–18** clustered tightly together (Table 2). The T_{50} s for these compounds exhibited a relatively narrow range (6190–7930 min) and were statistically similar.

In rat serum, the degradation profile of **14–18** was somewhat more widely distributed (T_{50} s ranging from 4070–9750 min) (Table 2). The rapid degradation of **13** resulted in the formation of a metabolite corresponding to the mass of the 9–13 fragment of **15**, consistent with cleavage at the Arg⁸–Arg⁹ site. Degradation products were generally not observed for the N-terminally capped Eisai compounds, even after the maximal assay period of 72 h. The high T_{50} s and lack of measurable degradation products demonstrate that the sequence modifications in the Eisai series effectively block serum enzymatic degradation at all susceptible sites in these compounds.

Table 2. Serum Degradation Rates, T_{50S}, and Major Metabolites Observed for Each Peptide Derivative in Human and Rat Serum

peptide	degradation rate ± SEM (μmol/min)		major degradation product ^a	half-time of disappearance (T ₅₀) ± SEM (min)	
	human	rat		human	rat
1	29.6 ± 0.68	49.8 ± 2.0	NT(9–13)	16.9 ± 0.05	10.0 ± 0.28
2	0.701 ± 0.01	2.38 ± 0.02	NT(8–11)	712 ± 9.6	210 ± 1.3
3	0.593 ± 0.01	1.92 ± 0.08	NT(8–11)	843 ± 19	260 ± 4.4
4	1.65 ± 0.01	3.53 ± 0.13	NT(8–11)	303 ± 5.0	141 ± 3.5
5	0.444 ± 0.01	2.28 ± 0.08	NT(8–11)	1130 ± 27	219 ± 6.4
6	2.17 ± 0.05	5.74 ± 0.16	NT(8–11)	230 ± 4.4	86.9 ± 1.5
7	33.4 ± 2.4	39.9 ± 3.6	KH28(9–13)	15.0 ± 0.12	12.6 ± 0.35
8	0.153 ± 0.01	0.146 ± 0.01	KH28(8–10)*	3270 ± 49	3420 ± 13
9	0.146 ± 0.01	0.117 ± 0.01	KH28(8–10)*	3430 ± 85	4310 ± 180
10	0.133 ± 0.01	0.160 ± 0.01	KH28(8–10)*	3760 ± 19	3120 ± 6.8
11	0.194 ± 0.01	0.166 ± 0.01	KH28(8–10)*	2570 ± 19	2980 ± 20
12	0.204 ± 0.01	0.111 ± 0.01	KH28(8–10)*	2460 ± 21	4490 ± 120
13	31.8 ± 0.34	37.0 ± 1.0	Eisai(9–13)	15.8 ± 0.36	13.5 ± 0.14
14	0.068 ± 0.01	0.089 ± 0.01	ND	7450 ± 320	5660 ± 320
15	0.068 ± 0.01	0.052 ± 0.01	ND	7390 ± 360	9750 ± 660
16	0.070 ± 0.01	0.123 ± 0.01	ND	7220 ± 290	4070 ± 23
17	0.064 ± 0.01	0.095 ± 0.01	ND	7930 ± 420	5270 ± 210
18	0.081 ± 0.01	0.078 ± 0.01	ND	6190 ± 240	6460 ± 300

^a Asterisks indicate that only trace amounts of material were observed at the corresponding molecular weights. ND = none detected.

Table 3. hNTR1 Binding data, EC₅₀ Values for Intracellular Ca²⁺ Mobilization, and Hypothermic Responses to ip Administration of NT(8–13), KH28, the Eisai Compound, and their N-Terminally Modified Analogues

peptide	IC ₅₀ (nM) ^a	K _i (nM) ^b	EC ₅₀ (nM) ^c	t _{max} (min) ^d	Δ in T _b (°C) ^{e,f}
NT	2.19 ± 0.5	1.64	1.98 ± 0.1		
haloperidol				90	-1.34 ± 0.10
1	1.40 ± 0.4	1.05	1.00 ± 0.2	300	-0.55 ± 0.14
2	2.42 ± 0.4	1.81	1.89 ± 0.1	90	-0.71 ± 0.30
3	0.383 ± 0.2	0.29	0.853 ± 0.1	120	-1.55 ± 0.15
4	0.970 ± 0.3	0.73	0.780 ± 0.2	240	-1.00 ± 0.24
5	6.50 ± 1.2	4.87	7.76 ± 1.5	150	-0.28 ± 0.12
6	2.68 ± 0.1	2.01	1.85 ± 0.2	120	-0.99 ± 0.16
7	10.8 ± 2.2	8.07	6.21 ± 1.3	90	-1.53 ± 0.14
8	181 ± 88	136	57.7 ± 2.7	150	-3.54 ± 0.24
9	27.0 ± 9.0	20.3	7.96 ± 3.0	180	-3.68 ± 0.24
10	7.32 ± 0.8	5.49	7.28 ± 3.0	120	-2.57 ± 0.12
11	13.9 ± 1.9	10.4	6.44 ± 1.8	150	-2.13 ± 0.09
12	3.99 ± 0.3	2.99	25.8 ± 3.1	90	-2.58 ± 0.20
13	403 ± 23	303	217 ± 23	120	-2.11 ± 0.23
14	863 ± 61	647	764 ± 250	270	-4.30 ± 0.21
15	240 ± 99	180	200 ± 49	270	-5.52 ± 0.33
16	140 ± 38	105	151 ± 16	240	-4.29 ± 0.42
17	2900 ± 610	2170	1860 ± 220	120	-4.28 ± 0.35
18	842 ± 200	631	783 ± 91	240	-5.02 ± 0.28

^a Concentration required to inhibit specific binding of ¹²⁵I-Tyr(3)[NT] (0.5 nM) to hNTR1 membrane preparations by 50%. Values are the mean of triplicate determinations ± SEM. ^b Calculated from mean IC₅₀ according to the Cheng–Prusoff equation³⁵ using a radioligand concentration of 0.5 nM and a K_d of 1.5 nM as given by the manufacturer. ^c Concentration required to elicit half-maximal intracellular Ca²⁺ mobilization in HT29 cells determined as described in the Experimental Section. Values are expressed as the mean of triplicate determinations ± SEM. ^d t_{max} (min) = time, in minutes, of maximal temperature decrease. ^e Δ in BT (°C) = Decrease in body temperature measured at t_{max}. Values are mean temperature decrease ± SEM. ^f Dose was 5 mg/kg (N = 5) for all peptides.

On the basis of the observed metabolites, the N-terminally unmodified peptides in each series (**1**, **7**, and **13**) degrade in the same fashion, through aminopeptidase cleavage between the Arg⁸ and Arg⁹ residues producing the corresponding 9–13 products (Table 2). In contrast, modification of the N-terminus by each of the functional groups in each peptide series completely prevented cleavage at the 8–9 amide bond. Instead, cleavage of the capped peptides shifted away from the N-terminus to alternative site(s) (Figure 1).

Compound **1** produces its biological effects through activation of G protein-coupled neurotensin receptors (NTRs).^{45,46} The NTR1 subtype binds **1** with high affinity and is thought to mediate its antipsychotic and hypothermic effects.^{47–49} To describe how the various N-terminal modifications affected interactions with a biological receptor, binding affinity and

agonism at hNTR1 were measured for each peptide derivative. Binding affinities of all peptides were determined based on their ability to compete with ¹²⁵I-Tyr(3)[NT] for binding to hNTR1 membrane preparations. IC₅₀ values determined from dose–response curves for each compound were converted to equilibrium dissociation constants (K_i values) according to the Cheng–Prusoff equation.³⁶

For the NT(8–13) peptide series, the various N-terminal modifications only modestly affected binding affinity (Table 3). K_i values for this series were comparable to that of unmodified **1** (1.05 nM). In fact, both the N^α-methyl (**3**) and azide (**4**) derivatives bound the receptor with slightly higher affinity than **1**. This suggests that hNTR1 tolerates both increased size and loss of the positive charge at this site. In contrast, **5** exhibited the lowest affinity of this series, suggesting that H-bonding at

the N-terminus of **1** plays a role in binding to hNTR1.⁵⁰ Loss of the free amine group in the **4**, **5**, and **6** derivatives would interrupt this H-bonding. Indeed, the des-amino derivative **6** gave the second highest K_i value in this series (Table 3). Replacement of the α -amine with a hydrogen atom results in maintenance of binding affinity even if H-bonding interaction is lost because no further steric bulk is introduced. Substitution of a methyl group at this position is apparently more disruptive, perhaps due to this hydrophobic moiety being placed too close to the polar residue(s) that take part in formation of endogenous H-bonds. While a similar situation might be expected for the azido functionality, it is possible that the increased size of the azido relative to the CH_3 - and H- groups is able to compensate for the loss of H-bonding by occupying a nearby pocket in the receptor that is not accessible by these other groups, as has been postulated for other peptide-receptor interactions.²⁷

For each N-terminal modification, the binding affinity was lower for the KH28 series when compared to their NT(8–13) counterparts. A number of differences exist between the binding affinity trends of these compounds (Table 3). For example, the N^α -acetylated **8** bound with the lowest affinity of this series, although acetylation had only a modest effect on binding for **2**. All of the other KH28 peptides exhibited K_i values similar to the unmodified **7**. Further, the C^α -methylated derivative (**11**), which had the least affinity for the receptor in the NT(8–13) series, was nearly as potent as **7**.

Binding affinity decreased further for each compound in the Eisai compared to the corresponding KH28 derivatives. However, the relationships observed within the Eisai series were very similar to those of the NT(8–13) series despite the fact that the Eisai compounds bound to hNTR1 with the overall lowest affinities (Table 3). This trend illustrates that it is the primary sequence of the peptide, not the N-terminal capping group that is the major contributor to binding affinity. As in the NT(8–13) series, compounds **15** and **16** bound more potently than the uncapped **13** and **17** exhibited markedly lower affinity. Thus, regardless of the differing primary sequences, the Eisai and NT(8–13) peptides appear to bind hNTR1 in a similar fashion.

The differences observed within the KH28 series suggest that the binding mode of the KH28 peptides may be subtly different from that of **1** and **15** and that the N-terminus of the KH28 derivatives may interact with different residues on the receptor. Within the KH28 series, the derivatives with the least polar, sterically least demanding N-terminal functionalities bind with the highest affinity. This trend indicates that steric and hydrophobic interactions are more important for the KH28 series and that H-bonding or electrostatic interactions are less important. Perhaps the polar nature and/or the added steric requirements of the N^α -acetyl- and, to a lesser extent, the C^α -methyl- functionalities impair the ability of the KH28 compounds to fit tightly into the active site of the receptor. The differences between the NT(8–13)/Eisai and KH28 series also suggest that the contribution to binding affinity for each N-terminal modification can differ based on the specific binding geometry/sequence of the peptide in which they are incorporated.

The K_i values for the KH28 and Eisai series increased about 1 and 2 orders of magnitude, respectively, relative to the NT(8–13) series (Table 3). These binding affinity data are in excellent agreement with previously reported values for **1** (0.14–1.0 nM),^{25,51–53} **10** (4.5 nM),²¹ **11** (9.9 nM),²² and **15** (95 nM),⁵³ which bear out a similar trend. The relatively moderate difference between the derivatives within each series indicates that the effect of the N-terminal modifications on binding affinity is relatively minimal.

Because **1**,⁵² **2**,⁵⁴ **10**,²¹ **11**,²² and **15**²⁶ are all known agonists at NTR1, it is reasonable to expect that the other analogues of **1** studied herein will behave as agonists as well. In the HT29 cell line, hNTR1 activation is coupled to the phosphoinositide cascade, leading to rapid liberation of intracellular Ca^{2+} stores.⁵⁴ This increase in intracellular Ca^{2+} concentration provides a convenient and easily monitored downstream effect of hNTR1 activation. The capacity of each N-terminally modified peptide to act as a functional agonist at hNTR1 was assessed by monitoring intracellular Ca^{2+} mobilization in HT29 cells. The peptide concentrations used in the experiment (1.0 pM to 1.0 μM) were chosen to bracket the known K_d value of NT (0.3 nM)⁵⁵ at NTR1 and the EC_{50} values for IP_3 production by NT and other NT derivatives with values in the nanomolar range.⁵⁴ EC_{50} values for each NT(8–13) analogue were determined from the resulting dose-response curves (Table 3).

The data demonstrate that each peptide acts as an agonist at hNTR1 because a transient increase in the concentration of free intracellular Ca^{2+} was observed in all cases. To show that the observed Ca^{2+} increases were due to activation of hNTR1, these experiments were repeated in the presence of SR48692 (**31**), a potent nonpeptide hNTR1 antagonist. Compound **31** competitively inhibits ¹²⁵I-labeled NT binding to hNTR1 with IC_{50} values ranging from 0.99–30.3 nM and also antagonizes several hNTR1 mediated signal transduction events, including intracellular Ca^{2+} mobilization^{56,57} (Figure S7, Supporting Information).

The NT(8–13) peptides were the most potent agonists, with EC_{50} values in the sub- to low nanomolar range (Table 3). N-terminal modification had only a modest effect on the potency of these compounds because the difference between the effectiveness of the most and least potent NT(8–13) peptides was less than 10-fold. Only **5** was significantly less effective at activating the receptor relative to the other derivatives. The KH28 peptides were less potent than those of the NT(8–13) series (Table 3). Again, the effect of the various N-terminal functional groups on potency was rather small as the range of potencies for the KH28 derivatives was also less than 10-fold. Continuing the trend of decreasing potency, the Eisai peptides were the least effective (Table 3). Within this series, the effects of the N-terminal modifications were also moderate (just over 12-fold) as only the effectiveness of **17** was significantly lower than the other peptides.

To a high degree, the functional agonism data paralleled those of the binding studies. Indeed, a plot of K_i vs EC_{50} revealed a close correlation ($r^2 = 0.98$) as would be expected for two interdependent parameters⁵⁴ (Figure S8, Supporting Information). A similar positive correlation has been observed in related studies.²⁶ One notable exception to this trend was **12**, which was the highest affinity KH28 derivative but was the second least potent agonist at hNTR1. Such disparities were not observed in the NT(8–13) or Eisai series. This could indicate that contacts made by the N-terminal functional group could be more crucial to receptor activation for the KH28 compounds and further supports the postulated alternative binding mode for KH28 derivatives. Within each series, the EC_{50} values for Ca^{2+} mobilization were generally within an order of magnitude of one another (Table 3). Thus, by analogy to the binding data, the decreases in potency across the peptide series are likely due to the primary sequence modifications and not the N-terminal modifications. The functional agonism data also compare favorably with previously determined EC_{50} values for NT in similar studies (2–5 nM).^{58–60}

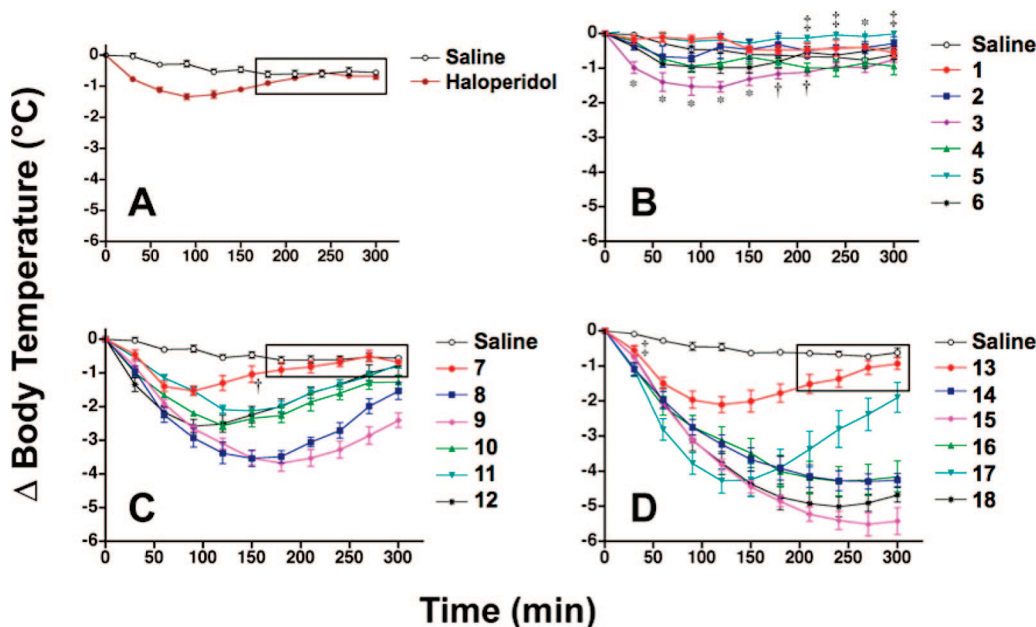


Figure 3. Decrease in core body temperature induced by peptides ip injected (5 mg/kg) into rats. (A) Haloperidol (5 mg/kg). (B) NT(8–13) series. (C) KH28 series. (D) Eisai series. Vertical bars indicate standard errors for each temperature ($n = 5$ for haloperidol and all peptides, $n = 10$ for saline controls). The boxed regions in (A), (C), and (D) indicate data points with no statistical significance ($p > 0.05$). All other points are significantly different from saline control at the $p < 0.001$ level unless otherwise indicated: * $p < 0.001$, † < 0.05 , ‡ < 0.01 . For clarity, only data points significantly different from saline control are labeled in (B).

NT, **1**, and a variety of NT(8–13) analogues exert a potent hypothermic effect following central administration.^{53,61–63} In contrast, reduction in body temperature is not observed upon peripheral NT administration, even at much higher concentrations than those that cause maximal effects after central infusion.^{61,64} Thus, NT-induced hypothermia is exclusively a result of central activity and can be used as marker to follow penetration of the blood–brain barrier (BBB) by NTR agonists. Knockout studies strongly suggest that the hypothermic response to NT is mediated by NTR1 because NTR1 knockout mice exhibited no hypothermia following administration of either NT (icv) or **15** (ip).^{48,49} Further, the structural elements of NT required to induce hypothermia parallel those found in SAR studies on binding potency at NTR1, suggesting that the same elements that mediate binding also mediate the hypothermic response.⁶² Therefore, hypothermia was used in this study as a direct measurement of a CNS effect triggered by the NTR1 receptor.

To assess how the various N-terminal modifications affected the ability of each peptide to enter the CNS and elicit a biological effect, core body temperature changes in rats were monitored following peripheral administration of each peptide derivative. Saline, haloperidol, or peptide were injected ip at a dose of 5.0 mg/kg into unanaesthetized, immobilized rats and rectal temperatures recorded over 5 h. Haloperidol, a typical antipsychotic drug, was included (also dosed at 5 mg/kg) as a representative of other clinically used neuroleptic agents. Relative to saline controls, haloperidol caused mild, but significant hypothermia for 150 min before returning to control levels. The maximal change in body temperature (ΔT_b) was -1.34 °C, in good agreement with previous reports,⁶⁵ and occurred at 90 min postinjection (Table 3 and Figure 3). Because of immobilization of the animals, the temperature of the rats receiving saline dropped by 0.5 °C on average over the course of the experiment as had been observed previously.⁶⁶

Compounds in the NT(8–13) series demonstrated poor hypothermic activity. Only **6** and **3** were able to elicit significant

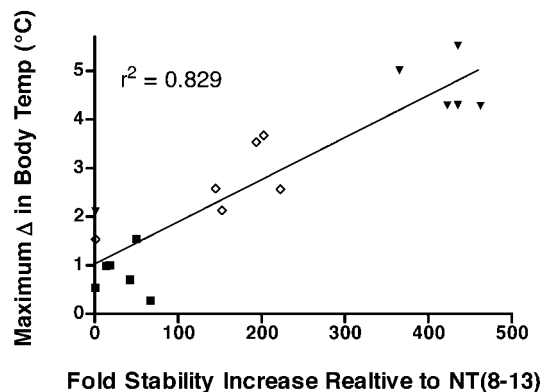


Figure 4. Correlation of stability and in vivo effect. Closed squares, NT(8–13) series; open diamonds, KH28 series; closed triangles, Eisai series.

hypothermic responses (Table 3 and Figure 3B). Compound **6** produced a slight short-lived hypothermic effect over the first hour of the time course while **3** caused significant hypothermia. Surprisingly, **5** caused weak, but significant, *hyper*thermia toward the end of the time course. None of the other derivatives of **1** generated effects on body temperature different from those of the saline controls (Figure 3B).

In contrast to the NT(8–13) series, each member of KH28 series elicited a significant hypothermic response (Table 3) and fairly similar time courses of activity (Figure 3C). Hypothermic activity was generally greatest in the Eisai series. Each of these compounds elicited a robust reduction in body temperature (Table 3 and Figure 3D) but significantly different time courses of activity, with **13** and **15** behaving like those of the KH28 series and **14**, and **16–18** exhibiting a much more pronounced and longer-lasting hypothermic effect.

Hypothermic potency of the three peptide series increased with enhanced stability: NT(8–13) < KH28 < Eisai, suggesting a strong relationship between these two parameters (Table 2). However, if stability alone was responsible for hypothermia one

would expect **5** and **2** to cause a significant hypothermic response because their degradation rates are close to that of **3**. Furthermore, **6**, the second least stable derivative, caused a small but significant decrease in body temperature (Figure 3B). Conversely, **4** was more stable than **6** but failed to reduce body temperature. The data suggest a complex interplay between stability, CNS access/retention, and binding affinity: the combination of high serum stability and high binding affinity/agonism undoubtedly contributed to the significant hypothermic effect elicited by **3**. However, its effect may have been augmented by increased transport across the BBB, reduced efflux, and/or low CNS metabolism. These parameters are likely to have distinguished **6** from the other derivatives as well, but its lower binding affinity/agonist activity are reflected in the smaller magnitude of the resultant hypothermia.

Because the main difference between the NT(8–13) and KH28 series is protection from EP 24.11 by the Tle substitution, this result underlines the importance of peripheral stability to the activity of these compounds. One interesting exception is the unmodified N-terminus of **7**. This compound is about as stable as **1** (Table 2) yet caused a 1.5 °C drop in rat body temperature equivalent to that of the most stable NT(8–13) compound (Figure 3). Given the lability of **7** to aminopeptidase attack in rat serum (Table 2), it is surprising that it was able to induce any significant response. This result suggests that at the relatively high dose used in this study, transient saturation of plasma aminopeptidases may occur, allowing a small amount of compound to enter the CNS and act before being degraded. Compounds **10**, **11**, and **12** all produce similar decreases in body temperature. While **11** and **10** have similar T_{50} values, **12** is significantly more stable (Table 2) and might be expected to yield a greater hypothermic response. The attenuated effect of this compound can be partially explained by its low agonist potency at hNTR1 (Table 3). Compounds **8** and **9** elicit just over 3.5 °C of hypothermia, but **8** is significantly less stable than **9**. Surprisingly, the acetylated derivative (**8**) also had the lowest binding affinity and was the poorest agonist of the series. Differences in central metabolism by EP 24.16 might explain this disparity.

The general correlation between peptide serum stability and hypothermic potency was maintained within the highly stable Eisai peptide series because these compounds caused the greatest hypothermia (Figure 3). Because compounds were the poorest in the NTR1 studies, it is obvious that binding and/or functional agonism at NTR1 are not the major influences of *in vivo* efficacy. Additionally, it is noted that peptides in both the NT(8–13) and Eisai series feature Arg at the N terminus, whereas the KH28 series compounds feature Hlys as the N-terminal residue. The same capping groups on Arg exhibit identical trends for both the *in vitro* and *in vivo* studies for the NT(8–13) and Eisai series. Thus, while the primary sequence between these two series affects the activity of the peptides with respect to binding and efficacy as discussed above, it is interesting that the capping groups produce the same trends of *in vitro* and *in vivo* effect when they are on the same amino acid, regardless the rest of the sequence.

Conclusion

Because the N-terminal modifications are equally effective at blocking aminopeptidase cleavage, one might expect that capping the N-terminus would result in a more or less equal degradation rate for the derivatives within each series. However, tightly clustered degradation profiles are not observed for the NT(8–13) and KH28 series. Peptides within these series exhibit

degradation rates with significantly different T_{50} values (Table 2). Because the N-terminal capping groups in this study differ with respect to sterics, charge, hydrophobicity, and H-bonding ability, it is reasonable to expect that they might also have different effects on the peptide binding conformation. Peptides with less than ~20 amino acids lack significant secondary structure but may adopt a particular conformation in the context of binding their biological targets.⁶⁷ It is also well established that cleavage efficiency at a particular site in a peptide can be drastically affected by modifications quite distant from the scissile bond. For example, DAP IV cleavage of GRF(1–29) occurs between residues 2 and 3, yet hydrolysis at this site was inhibited by modifications as far away as residue 25.⁶⁸ Such long-distance effects must be the result of changes in the overall peptide conformation to inhibit the action of enzymes sensitive to local structure. Similar effects have also been reported for smaller peptides, where substitution of certain natural and non-natural L- and D-amino acids at positions removed from a cleavage site impacts the stability of the hydrolyzed bond.^{12,14} Further, simple N-terminal modifications, including N^{α} -methylation, can also dramatically modify peptide structure and thereby alter the accessibility of susceptible sites to peptidases.^{19,69} Thus, it is likely that the degradation rate differences are due to N-terminal specific alterations in the population of peptide conformers that maintain the correct geometry for interaction with proteolytic enzymes.

Interestingly, the modifications studied are not intrinsically detrimental to hNTR1 binding because the binding affinity differences between the derivatives within each series were relatively small (Table 3). Obviously, the N-terminus of each NT(8–13) analogue is amenable to both steric and electrostatic modifications because compounds bearing bulkier and uncharged functionalities at the N-terminus bind more efficiently than the unmodified peptide in each case. Similar results have been reported in other studies where N-terminal acetylation and other N-terminal modifications of **1** did not adversely effect binding affinity.^{51,54,70–72} While none of the N-terminal modifications significantly improved the efficacy of receptor activation, many maintained functional agonism at unmodified levels. The N-terminal modifications used in these peptides may have specific effects depending on the primary peptide sequence but clearly have the potential to improve the PK properties of peptides overall without adversely affecting binding affinity and receptor potency.

Decrease in body temperature following peripheral administration of the peptides demonstrates that the compounds are able to enter the CNS from the periphery and elicit a biological effect mediated by NTR1. Entry into the CNS is a major obstacle that must be overcome in order for NT(8–13) analogues to produce hypothermia. The BBB suppresses paracellular diffusion across the brain capillaries and is enriched in a number of peptidases, particularly aminopeptidases.⁷³ Because the peptide compounds in this study are quite polar and of relatively high molecular weight, it is unlikely that they cross the BBB by passive diffusion.⁷⁴ Thus, the central activity of the peptides implies that they traverse the BBB via active transport. Indeed, transport via a saturable system has been reported for **15**⁷⁵ and suggested in related studies.⁷⁶ To assert hypothermic activity, NT(8–13) analogues must be stable enough to reach and cross the BBB. Thus, the relative level of stability is likely to be the principal determinant of hypothermic potency. However, once this stability threshold is reached, other secondary factors such as BBB influx/efflux, CNS metabolism, and binding potency become important. Differences in enzymatic metabolism due

to the effects of N-terminal modification were suggested by the serum degradation data. It is reasonable that similar differences might exist between the derivatives with respect to cleavage by EP 24.16 once the peptides enter the brain. Differences in CNS metabolism also could help explain the lack of central effect for **4**, **2**, and **5**.

Why do highly stable peptide molecules exert a more potent physiological effect when their receptor binding affinities are more than 3 orders of magnitude lower than related less potent compounds? This phenomenon may represent increased bioavailability of the stable analogues, either through increased brain uptake, altered peripheral pharmacokinetics, or a combination thereof. Because the N-terminal modifications dramatically improve peptide stability, a given concentration of peptide is exposed to the capillary endothelial cell surface of the BBB for a longer period of time, leading to greater penetration and higher central activity. Because the maximal brain uptake of a peptide is directly proportional to its plasma profile,⁷⁴ the more stable peptides are hypothesized to have greater CNS access as has been observed for NT(8–13) derivatives and other peptide systems.^{3,77}

Modifications in the primary sequence of **1** reduced binding affinity and functional agonism at NTR1, however, the N-terminal modifications were not inherently detrimental to either of these properties (Table 3). In fact, N-terminally modified derivatives within each peptide series bound to and activated the receptor with greater affinity/potency than the corresponding uncapped parent peptides. Interestingly, no obvious trends with respect to the rank orders of the N-terminal functional groups were apparent across the stability, binding, and agonist studies, suggesting complex sequence-specific interactions with the N-terminus of each peptide. Whereas NTR1 binding was directly proportional to functional agonism, this is not the case with hypothermic effect. Surprisingly, stability, but not receptor binding affinity or agonism, correlated with the extent of hypothermia (Figure 4). Although the most stable peptides exhibited the lowest binding affinities and were the least potent agonists, they produced the largest decreases in body temperature as well as the most prolonged effects. This relationship demonstrates that a reduction in binding affinity at NTR1 can be countered by increased in vivo stability.

A number of efficacious NT(8–13) analogues have been reported that exhibit weak binding to the NTRs. Invariably, each of these analogues was a stabilized derivative.^{47,51,53,63,78–80} Likewise, several examples of NT(8–13) analogues have been reported in which binding affinity is improved but efficacy is lost.⁸⁰ In each of these cases, stability tracks closely with the observed biological effect and appears to be the key parameter influencing efficacy. This effect has been observed in other peptide systems. For example, addition of PEG to a Met-enkephalin analogue decreased binding affinity for the δ -opioid receptor by 172-fold but increased both its stability and analgesic effect.³ Neuromedin N (NN), a neuropeptide closely related in structure to NT, is uncapped, highly unstable in vivo, and produces no central effects following peripheral administration.⁸¹ However, coadministration of the aminopeptidase inhibitor bestatin allows NN to elicit a robust hypothermic response, again illustrating the importance of stability to elicit its effect.

The current study provides a direct comparison between various commonly used and novel N-terminal functionalities as capping groups and demonstrates that peptide stability is more important to in vivo efficacy than receptor binding affinity or functional receptor agonism in the NT(8–13) system. However, because the uncapped (and unstable) **7** and **13** compounds were

able to cause significant biological responses, stability alone is not sufficient to explain all of the observed effects. While stability is clearly the dominant parameter for these peptides, N-terminal modification likely altered a number of other properties including hydrophobicity, elimination half-life, and BBB transport, the combination of which resulted in an improved hypothermic effect. Further, it is apparent that judicious selection of N-terminal capping moieties also can lead to enhancement of barrier crossing and other parameters relevant to peptide-based therapeutics.

Acknowledgment. This work was supported by NIH grants MH-65099 and GM-70044 (T.A.D., PI). K.S.O. and M.K.H. are AFPE predoctoral scholars. The MUSC NMR and mass spectrometry facilities were used as part of this work. We thank Dr. Mark Busman for many helpful discussions and expert mass spectral support and acknowledge Dr. John Oatis for assistance with NMR experiments. The SR48692 was a generous gift from Sanofi Research. We thank Dr. Yurii Mukhin for assistance with the FLIPR instrument, which was supported by NIH grant 1S10RR013005-01. This work was conducted in a facility constructed with support from the National Institute of Health, Grant Number C06RR015455 from the Extramural Research Facilities Program of the National Center for Research Resources.

Supporting Information Available: General experimental procedures; synthesis schemes 1–4; serum degradation standard curves; analytical data and experimental procedures for compounds **19**, **22**, **25**, and **28**; analytical HPLC analysis and MALDI-TOF data for each of the target peptides. This material is available free of charge via the Internet at <http://pubs.acs.org>.

References

- (1) Lee, H. J. Biopharmaceutical Properties and Pharmacokinetics of Peptide and Protein Drugs. In *Peptide-Based Drug Design: Controlling Transport and Metabolism*; Taylor, M. D., Amidon, G. L., Eds.; American Chemical Society: Washington, DC, 1995; pp 69–97.
- (2) Egleton, R. D.; Mitchell, S. A.; Huber, J. D.; Palian, M. M.; Polt, R.; Davis, T. P. Improved blood–brain barrier penetration and enhanced analgesia of an opioid peptide by glycosylation. *J. Pharmacol. Exp. Ther.* **2001**, *299* (3), 967–972.
- (3) Witt, K. A.; Huber, J. D.; Egleton, R. D.; Roberts, M. J.; Bentley, M. D.; Guo, L.; Wei, H.; Yamamura, H. I.; Davis, T. P. Pharmacodynamic and pharmacokinetic characterization of poly(ethylene glycol) conjugation to met-enkephalin analog [D-Pen2, D-Pen5]-enkephalin (DPDPE). *J. Pharmacol. Exp. Ther.* **2001**, *298* (2), 848–856.
- (4) Borchardt, R. T. Optimizing oral absorption of peptides using prodrug strategies. *J. Controlled Release* **1999**, *62* (1–2), 231–238.
- (5) Wen, J. J.; Crews, C. M. Synthesis of 9-fluorenylmethoxycarbonyl-protected amino aldehydes. *Tetrahedron: Asymmetry* **1998**, *9* (11), 1855–1858.
- (6) Gupta, S.; Payne, J. W. Evaluation of the conformational propensities of peptide isosteres as a basis for selecting bioactive pseudopeptides. *J. Pept. Res.* **2001**, *58* (6), 546–561.
- (7) Miwa, J. H.; Patel, A. K.; Vivatrat, N.; Popek, S. M.; Meyer, A. M. Compatibility of the Thioamide Functional Group with β -Sheet Secondary Structure: Incorporation of a Thioamide Linkage into a β -Hairpin Peptide. *Org. Lett.* **2001**, *3* (21), 3373–3375.
- (8) Lee, H.-J.; Song, J.-W.; Choi, Y.-S.; Park, H.-M.; Lee, K.-B. A Theoretical Study of Conformational Properties of N-Methyl Azapeptide Derivatives. *J. Am. Chem. Soc.* **2002**, *124* (40), 11881–11893.
- (9) Guichard, G. Beta-Peptides, Gamma-Peptides, and Isoelectric Backbones: New Scaffolds with Controlled Shapes for Mimicking Protein Secondary Structure Elements. In *Pseudo-Peptides in Drug Discovery*; Nielsen, P. E., Ed.; Wiley-VCH: Weinheim, Germany, 2004; pp 33–120.
- (10) Patch, J. A.; Kirshenbaum, K.; Seurnyck, S. L.; Zuckermann, R. N.; Barron, A. E. Versatile Oligo(N-Substituted) Glycines: The Many Roles of Peptoids in Drug Discovery. In *Pseudo-Peptides in Drug Discovery*; Nielsen, P. E., Ed.; Wiley-VCH: Weinheim, Germany, 2004; pp 1–31.
- (11) Sawyer, T. K. Peptidomimetic Design and Chemical Approaches to Peptide Metabolism. In *Peptide-Based Drug Design: Controlling Transport and Metabolism*; Taylor, M. D., Amidon, G. L., Eds.; American Chemical Society: Washington, DC, 1995; pp 387–422.

- (12) Delange, R. J.; Smith, E. L., Leucine Aminopeptidase and Other N-Terminal Exopeptidases. In *The Enzymes*, 3rd ed.; Boyer, P. D., Ed.; Academic Press: New York, 1971; Vol. 3, pp 81–118.
- (13) Lugrin, D.; Vecchini, F.; Doulet, S.; Rodriguez, M.; Martinez, J.; Kitabgi, P. Reduced peptide bond pseudopeptide analogues of neurotensin: binding and biological activities, and in vitro metabolic stability. *Eur. J. Pharmacol.* **1991**, *205* (2), 191–198.
- (14) Heavner, G. A.; Kroon, D. J.; Audhya, T.; Goldstein, G. Biologically active analogs of thymopentin with enhanced enzymatic stability. *Peptides* **1986**, *7* (6), 1015–1019.
- (15) Powell, M. F. Peptide stability in drug development: in vitro peptide degradation in plasma and serum. *Annu. Rep. Med. Chem.* **1993**, *28*, 285–294.
- (16) Driessen, H. P.; Ramaekers, F. C.; Vree Egberts, W. T.; Dodemont, H. J.; de Jong, W. W.; Tesser, G. I.; Bloemendal, H. The function of N alpha-acetylation of the eye-lens crystallins. *Eur. J. Biochem.* **1983**, *136* (2), 403–406.
- (17) Stock, A.; Clarke, S.; Clarke, C.; Stock, J. N-Terminal methylation of proteins: structure, function and specificity. *FEBS Lett.* **1987**, *220* (1), 8–14.
- (18) Bajusz, S.; Szell, E.; Bagdy, D.; Barabas, E.; Horvath, G.; Dioszegi, M.; Fittler, Z.; Szabo, G.; Juhasz, A.; Tomori, E.; et al. Highly active and selective anticoagulants: D-Phe-Pro-Arg-H, a free tripeptide aldehyde prone to spontaneous inactivation, and its stable N-methyl derivative, D-MePhe-Pro-Arg-H. *J. Med. Chem.* **1990**, *33* (6), 1729–1735.
- (19) Marschutz, M. K.; Zauner, W.; Mattner, F.; Otava, A.; Buschle, M.; Bernkop-Schnurch, A. Improvement of the enzymatic stability of a cytotoxic T-lymphocyte-epitope model peptide for its oral administration. *Peptides* **2002**, *23* (10), 1727–1733.
- (20) Lundquist, J. T. I. V.; Dix, T. A. Synthesis and human neurotensin receptor binding activities of Neurotensin(8–13) analogs containing position 8 a-azido-N-alkylated derivatives of ornithine, lysine, and homolysine. *J. Med. Chem.* **1999**, *42* (23), 4914–4918.
- (21) Kokko, K. P.; Hadden, M. K.; Orwig, K. S.; Mazella, J.; Dix, T. A. In vitro analysis of stable, receptor-selective neurotensin(8–13) analogues. *J. Med. Chem.* **2003**, *46* (19), 4141–4148.
- (22) Hadden, M. K.; Orwig, K. S.; Kokko, K. P.; Mazella, J.; Dix, T. A. Design, synthesis, and evaluation of the antipsychotic potential of orally bioavailable neurotensin(8–13) analogues containing non-natural arginine and lysine residues. *Neuropharmacology* **2005**, *49* (8), 1149–1159.
- (23) Boules, M.; Shaw, A.; Fredrickson, P.; Richelson, E. Neurotensin agonists: potential in the treatment of schizophrenia. *CNS Drugs* **2007**, *21* (1), 13–23.
- (24) Dobner, P. R. Neurotensin and pain modulation. *Peptides* **2006**, *27* (10), 2405–2414.
- (25) Okarvi, S. M. Peptide-based radiopharmaceuticals and cytotoxic conjugates: potential tools against cancer. *Cancer Treat. Rev.* **2008**, *34* (1), 13–26.
- (26) Akunne, H. C.; Demattos, S. B.; Whetzel, S. Z.; Wustrow, D. J.; Davis, D. M.; Wise, L. D.; Cody, W. L.; Pugsley, T. A.; Heffner, T. G. Agonist properties of a stable hexapeptide analog of neurotensin, N alpha MeArg-Lys-Pro-Trp-tLeu-Leu (NT1). *Biochem. Pharmacol.* **1995**, *49* (8), 1147–1154.
- (27) Kennedy, K. J.; Orwig, K. S.; Dix, T. A.; Christopher, J.; Jaffa, A. A. Synthesis and analysis of potent, more lipophilic derivatives of the bradykinin B2 receptor antagonist peptide Hoe 140. *J. Pept. Res.* **2002**, *59* (4), 139–148.
- (28) Carpino, L. A.; Han, G. Y. 9-Fluorenylmethoxycarbonyl amino-protecting group. *J. Org. Chem.* **1972**, *37* (22), 3404–3409.
- (29) Kennedy, K. J.; Lundquist, I.; Joseph, T.; Simandan, T. L.; Beeson, C. C.; Dix, T. A. Asymmetric synthesis of non-natural homologues of lysine. *Bioorg. Med. Chem. Lett.* **1997**, *7* (14), 1937–1940.
- (30) Orwig, K. S.; Dix, T. A. Synthesis of C-alpha methylated carboxylic acids: isosteres of arginine and lysine for use as N-terminal capping residues in polypeptides. *Tetrahedron Lett.* **2005**, *46* (41), 7007–7009.
- (31) Lundquist, J. T. I. V.; Pelletier, J. C. Improved solid-phase peptide synthesis method utilizing a-azide-protected amino acids. *Org. Lett.* **2001**, *3* (5), 781–783.
- (32) Evans, D. A.; Britton, T. C.; Ellman, J. A. Contrasteric carboximide hydrolysis with lithium hydroperoxide. *Tetrahedron Lett.* **1987**, *28* (49), 6141–6144.
- (33) Lee, H.-S.; LePlae, P. R.; Porter, E. A.; Gellman, S. H. An Efficient Route to Either Enantiomer of Orthogonally Protected *trans*-3-Aminopyrrolidine-4-carboxylic Acid. *J. Org. Chem.* **2001**, *66* (10), 3597–3599.
- (34) Miller, S. C.; Scanlan, T. S. Site-Selective N-Methylation of Peptides on Solid Support. *J. Am. Chem. Soc.* **1997**, *119* (9), 2301–2302.
- (35) Kokko, K. P.; Dix, T. A. Monitoring neurotensin(8–13) degradation in human and rat serum utilizing matrix-assisted laser desorption/ionization time-of-flight mass spectrometry. *Anal. Biochem.* **2002**, *308* (1), 34–41.
- (36) Cheng, Y.; Prusoff, W. H. Relationship between the inhibition constant (K_i) and the concentration of inhibitor which causes 50% inhibition (IC_{50}) of an enzymatic reaction. *Biochem. Pharmacol.* **1973**, *22* (23), 3099–3108.
- (37) Aronin, N.; Carraway, R. E.; Ferris, C. F.; Hammer, R. A.; Leeman, S. E. The stability and metabolism of intravenously administered neurotensin in the rat. *Peptides* **1982**, *3* (4), 637–642.
- (38) Lee, Y. C.; Uttenthal, L. O.; Smith, H. A.; Bloom, S. R. In vitro degradation of neurotensin in human plasma. *Peptides* **1986**, *7* (3), 383–387.
- (39) Checler, F.; Barelli, H.; Kitabgi, P.; Vincent, J. P. Neurotensin metabolism in various tissues of central and peripheral origins: ubiquitous involvement of a novel neurotensin degrading metalloendopeptidase. *Biochimie* **1988**, *70* (1), 75–82.
- (40) Checler, F.; Vincent, J. P.; Kitabgi, P. Inactivation of neurotensin by rat brain synaptic membranes partly occurs through cleavage at the Arg8–Arg9 peptide bond by a metalloendopeptidase. *J. Neurochem.* **1985**, *45* (5), 1509–1513.
- (41) Checler, F.; Vincent, J. P.; Kitabgi, P. Degradation of neurotensin by rat brain synaptic membranes: involvement of a thermolysin-like metalloendopeptidase (enkephalinase), angiotensin-converting enzyme, and other unidentified peptidases. *J. Neurochem.* **1983**, *41* (2), 375–384.
- (42) McDermott, J. R.; Smith, A. I.; Edwardson, J. A.; Griffiths, E. C. Mechanism of neurotensin degradation by rat brain peptidases. *Regul. Pept.* **1982**, *3* (5–6), 397–404.
- (43) Bruehlmeier, M.; Garayoa, E. G.; Blanc, A.; Holzer, B.; Gergely, S.; Tourwe, D.; Schubiger, P. A.; Blauenstein, P. Stabilization of neurotensin analogues: effect on peptide catabolism, biodistribution and tumor binding. *Nuclear Med. Biol.* **2002**, *29* (3), 321–327.
- (44) Garcia-Garayoa, E.; Allemann-Tannahill, L.; Blauenstein, P.; Willmann, M.; Carrel-Remy, N.; Tourwe, D.; Iterbeke, K.; Conrath, P.; Schubiger, P. A. In vitro and in vivo evaluation of new radiolabeled neurotensin(8–13) analogues with high affinity for NT1 receptors. *Nucl. Med. Biol.* **2001**, *28* (1), 75–84.
- (45) Vincent, J. P. Neurotensin receptors: binding properties, transduction pathways, and structure. *Cell. Mol. Neurobiol.* **1995**, *15* (5), 501–512.
- (46) Vincent, J. P.; Mazella, J.; Kitabgi, P. Neurotensin and neurotensin receptors. *Trends Pharmacol. Sci.* **1999**, *20* (7), 302–309.
- (47) Dubuc, I.; Sarret, P.; Labbe-Julie, C.; Botto, J. M.; Honore, E.; Bourdel, E.; Martinez, J.; Costentin, J.; Vincent, J. P.; Kitabgi, P.; Mazella, J. Identification of the receptor subtype involved in the analgesic effect of neurotensin. *J. Neurosci.* **1999**, *19* (1), 503–510.
- (48) Pettibone, D. J.; Hess, J. F.; Hey, P. J.; Jacobson, M. A.; Leviten, M.; Lis, E. V.; Mallorga, P. J.; Pascarella, D. M.; Snyder, M. A.; Williams, J. B.; Zeng, Z. The effects of deleting the mouse neurotensin receptor NTR1 on central and peripheral responses to neurotensin. *J. Pharmacol. Exp. Ther.* **2002**, *300* (1), 305–313.
- (49) Remaury, A.; Vita, N.; Gendreau, S.; Jung, M.; Arnone, M.; Poncelet, M.; Culouscou, J. M.; Le Fur, G.; Soubrie, P.; Caput, D.; Shire, D.; Kopf, M.; Ferrara, P. Targeted inactivation of the neurotensin type 1 receptor reveals its role in body temperature control and feeding behavior but not in analgesia. *Brain Res.* **2002**, *953* (1–2), 63–72.
- (50) Bouvier, M.; Guo, H. C.; Smith, K. J.; Wiley, D. C. Crystal structures of HLA-A*0201 complexed with antigenic peptides with either the amino- or carboxyl-terminal group substituted by a methyl group. *Proteins* **1998**, *33* (1), 97–106.
- (51) Kitabgi, P.; Poustis, C.; Granier, C.; Van Rietschoten, J.; Rivier, J.; Morgat, J. L.; Freychet, P. Neurotensin binding to extraneural and neural receptors: comparison with biological activity and structure–activity relationships. *Mol. Pharmacol.* **1980**, *18* (1), 11–19.
- (52) Mills, A.; Demoliou-Mason, C. D.; Barnard, E. A. Characterization of neurotensin binding sites in intact and solubilized bovine brain membranes. *J. Neurochem.* **1988**, *50* (3), 904–911.
- (53) Tyler, B. M.; Douglas, C. L.; Fauq, A.; Pang, Y. P.; Stewart, J. A.; Cusack, B.; McCormick, D. J.; Richelson, E. In vitro binding and CNS effects of novel neurotensin agonists that cross the blood–brain barrier. *Neuropharmacology* **1999**, *38* (7), 1027–1034.
- (54) Amar, S.; Kitabgi, P.; Vincent, J. P. Activation of phosphatidylinositol turnover by neurotensin receptors in the human colonic adenocarcinoma cell line HT29. *FEBS Lett.* **1986**, *201* (1), 31–36.
- (55) Vincent, J. P.; Mazella, J.; Kitabgi, P. Neurotensin and neurotensin receptors. *Trends Pharmacol. Sci.* **1999**, *20* (7), 302–309.
- (56) Gully, D.; Canton, M.; Boigegrain, R.; Jeanjean, F.; Molimard, J. C.; Poncelet, M.; Gueudet, C.; Heulme, M.; Leyris, R.; Brouard, A.; et al. Biochemical and pharmacological profile of a potent and selective nonpeptide antagonist of the neurotensin receptor. *Proc. Natl. Acad. Sci. U.S.A.* **1993**, *90* (1), 65–69.
- (57) Oury-Donat, F.; Thurneyssen, O.; Gonalons, N.; Forgez, P.; Gully, D.; Le Fur, G.; Soubrie, P. Characterization of the effect of SR48692 on inositol monophosphate, cyclic GMP and cyclic AMP responses linked to neurotensin receptor activation in neuronal and non-neuronal

- cells. *Br. J. Pharmacol.* **1995**, *116* (2), 1899–1905.
- (58) Snider, R. M.; Forray, C.; Pfenning, M.; Richelson, E. Neurotensin stimulates inositol phospholipid metabolism and calcium mobilization in murine neuroblastoma clone N1E-115. *J. Neurochem.* **1986**, *47* (4), 1214–1218.
- (59) Bozou, J. C.; Rochet, N.; Magnaldo, I.; Vincent, J. P.; Kitabgi, P. Neurotensin stimulates inositol trisphosphate-mediated calcium mobilization but not protein kinase C activation in HT29 cells. Involvement of a G-protein. *Biochem. J.* **1989**, *264* (3), 871–878.
- (60) Ryder, N. M.; Guha, S.; Hines, O. J.; Reber, H. A.; Rozengurt, E. G protein-coupled receptor signaling in human ductal pancreatic cancer cells: neurotensin responsiveness and mitogenic stimulation. *J. Cell. Physiol.* **2001**, *186* (1), 53–64.
- (61) Bisette, G.; Nemeroff, C. B.; Loosen, P. T.; Prange, A. J., Jr.; Lipton, M. A. Hypothermia and intolerance to cold induced by intracisternal administration of the hypothalamic peptide neurotensin. *Nature* **1976**, *262* (5569), 607–609.
- (62) Loosen, P. T.; Nemeroff, C. B.; Bisette, G.; Burnett, G. B.; Prange, A. J., Jr.; Lipton, M. A. Neurotensin-induced hypothermia in the rat: structure-activity studies. *Neuropharmacology* **1978**, *17* (2), 109–113.
- (63) Rivier, J. E.; Lazarus, L. H.; Perrin, M. H.; Brown, M. R. Neurotensin analogues. Structure–activity relationships. *J. Med. Chem.* **1977**, *20* (11), 1409–1412.
- (64) Bisette, G.; Luttinger, D.; Mason, G. A.; Hernandez, D. E.; Loosen, P. T. Neurotensin and thermoregulation. *Ann. N.Y. Acad. Sci.* **1982**, *400*, 268–282.
- (65) Hamuro, A.; Miyaoka, H.; Iguchi, T.; Kamijima, K. Hypothermia developing during neuroleptic treatment. *Pharmacopsychiatry* **1999**, *32* (6), 258–259.
- (66) Kokko, K. P.; Hadden, M. K.; Price, K. L.; Orwig, K. S.; See, R. E.; Dix, T. A. In vivo behavioral effects of stable, receptor-selective neurotensin(8–13) analogues that cross the blood–brain barrier. *Neuropharmacology* **2005**, *48* (3), 417–425.
- (67) Sabo, T. M.; Farrell, D. H.; Maurer, M. C. Conformational Analysis of γ' Peptide (410–427) Interactions with Thrombin Anion Binding Exosite II. *Biochemistry* **2006**, *45* (24), 7434–7445.
- (68) Su, C. M.; Jensen, L. R.; Heimer, E. P.; Felix, A. M.; Pan, Y. C.; Mowles, T. F. In vitro stability of growth hormone releasing factor (GRF) analogs in porcine plasma. *Horm. Metab. Res.* **1991**, *23* (1), 15–21.
- (69) Turker, R. K.; Ercan, Z. S. Change of activity in rabbit aorta of three analogs of angiotensin substituted in nh2-terminal position. *Pharmacology* **1975**, *13* (2), 155–162.
- (70) Reubi, J. C.; Waser, B.; Friess, H.; Buchler, M.; Laissue, J. Neurotensin receptors: a new marker for human ductal pancreatic adenocarcinoma. *Gut* **1998**, *42* (4), 546–550.
- (71) Labbe-Julie, C.; Dubuc, I.; Brouard, A.; Doulut, S.; Bourdel, E.; Pelaprat, D.; Mazella, J.; Martinez, J.; Rostene, W.; Costentin, J.; et al. In vivo and in vitro structure–activity studies with peptide and pseudopeptide neurotensin analogs suggest the existence of distinct central neurotensin receptor subtypes. *J. Pharmacol. Exp. Ther.* **1994**, *268* (1), 328–336.
- (72) Bergmann, R.; Scheunemann, M.; Heichert, C.; Mading, P.; Wittirsch, H.; Kretzschmar, M.; Rodig, H.; Tourwe, D.; Itebeke, K.; Chavatte, K.; Zips, D.; Reubi, J. C.; Johannsen, B. Biodistribution and catabolism of (18)F-labeled neurotensin(8–13) analogs. *Nucl. Med. Biol.* **2002**, *29* (1), 61–72.
- (73) Brownlees, J.; Williams, C. H. Peptidases, peptides, and the mammalian blood–brain barrier. *J. Neurochem.* **1993**, *60* (3), 793–803.
- (74) Pardridge, W. M. CNS drug design based on principles of blood–brain barrier transport. *J. Neurochem.* **1998**, *70* (5), 1781–1792.
- (75) Banks, W. A.; Wustrow, D. J.; Cody, W. L.; Davis, M. D.; Kastin, A. J. Permeability of the blood–brain barrier to the neurotensin8–13 analog NT1. *Brain Res.* **1995**, *695* (1), 59–63.
- (76) Hadden, M. K.; Walle, T.; Dix, T. A. Cellular uptake of a radiolabelled analogue of neurotensin in the Caco-2 cell model. *J. Pharm. Pharmacol.* **2005**, *57* (3), 327–333.
- (77) Egleton, R. D.; Davis, T. P. Bioavailability and transport of peptides and peptide drugs into the brain. *Peptides* **1997**, *18* (9), 1431–1439.
- (78) Gilbert, J. A.; Moses, C. J.; Pfenning, M. A.; Richelson, E. Neurotensin and its analogs—correlation of specific binding with stimulation of cyclic GMP formation in neuroblastoma clone N1E-115. *Biochem. Pharmacol.* **1986**, *35* (3), 391–397.
- (79) Gilbert, J. A.; McCormick, D. J.; Pfenning, M. A.; Kanba, K. S.; Enloe, L. J.; Moore, A.; Richelson, E. Neurotensin(8–13): comparison of novel analogs for stimulation of cyclic GMP formation in neuroblastoma clone N1E-115 and receptor binding to human brain and intact N1E-115 cells. *Biochem. Pharmacol.* **1989**, *38* (19), 3377–3382.
- (80) Heyl, D. L.; Seffler, A. M.; He, J. X.; Sawyer, T. K.; Wustrow, D. J.; Akunne, H. C.; Davis, M. D.; Pugsley, T. A.; Heffner, T. G.; Corbin, A. E.; et al. Structure–activity and conformational studies of a series of modified C-terminal hexapeptide neurotensin analogues. *Int. J. Pept. Protein Res.* **1994**, *44* (3), 233–238.
- (81) Dubuc, I.; Nouel, D.; Coquerel, A.; Menard, J. F.; Kitabgi, P.; Costentin, J. Hypothermic effect of neuromedin N in mice and its potentiation by peptidase inhibitors. *Eur. J. Pharmacol.* **1988**, *151* (1), 117–121.

JM801072V